Contribution from the Department of Chemistry, Rice University, Houston, Texas 77251, Department of Chemistry, University of Delaware, Newark, Delaware 19716, and the INC4 Division of Los Alamos National Laboratory, Los Alamos, New Mexico 87545

A Series of Thallium–Iron Carbonyl Cluster Molecules: Structural Comparisons of $[Et_4N]_2[Tl_2Fe_4(CO)_{16}]$, $[Et_4N]_4[Tl_4Fe_8(CO)_{30}]$, and $[Et_4N]_6[Tl_6Fe_{10}(CO)_{36}]$

Kenton H. Whitmire,*† Juanita M. Cassidy,† A. L. Rheingold,‡ and Robert R. Ryan§

Received September 22, 1987

Thallium salts and in situ generated $K^+[HFe(CO)_4]^-$ react to form $K^+[Tl\{Fe(CO)_4\}_2]$. The $[Et_4N]^+$ salt exists as a dimer in the solid state. Single-crystal X-ray analysis of $[Et_4N]_2[Tl_2Fe_4(CO)_{16}]$ ($[Et_4N]_2[I]$) shows it to crystallize in the triclinic, centrosymmetric space group $P\bar{1}$ with a = 11.00 (1) Å, b = 12.98 (1) Å, c = 8.77 (1) Å, α = 105.3 (1)°, β = 95.7 (1)°, γ = 65.30 (8)°, Z = 1, and V = 1097 Å^3. The dimerization occurs through the formation of an asymmetric Tl_2Fe_2 parallelogram with Tl–Fe distances of 2.632 (5) and 3.038 (4) Å. The Fe atoms in the parallelogram are pseudooctahedrally coordinated by the two thallium atoms and four carbonyls. The remaining $Fe(CO)_4$ groups are trigonal bipyramids with thalliums located in axial sites (d_{Tl-Fe} = 2.553 (5) Å). $[Et_4N]_2[I]$ is monomeric in solution and loses CO upon standing or irradiation to produce $[Et_4N]_4[Tl_4Fe_8(CO)_{30}]$ ($[Et_4N]_4[II]$), which has also been characterized by single-crystal X-ray diffraction: monoclinic space group $P2_1/n$, with a = 12.723 (6) Å, b = 16.077 (6) Å, c = 21.430 (9) Å, β = 95.97 (4)°, Z = 2, and V = 4360.2 Å^3. It too contains a Tl_2Fe_2 parallelogram with d_{Tl-Fe} = 2.781 (5) and 2.786 (6) Å. In addition those two thalliums bridge $Fe_2(CO)_6(\mu\text{-}CO)(\mu\text{-}TlFe(CO)_4)$ groups. The CO loss reaction is reversible under pressures of CO. Structural comparisons are made of $[Et_4N]_2[I]$ and $[Et_4N]_4[II]$ to the previously reported $[Et_4N]_4[Tl_6Fe_{10}(CO)_{36}]$ ($[Et_4N]_4[III]$): monoclinic space group $P2_1/n$, with a = 12.266 (5) Å, b = 20.547 (3) Å, c = 22.892 (6) Å, β = 93.24 (3)°, Z = 2, and V = 5759.7 Å^3.

Introduction

Homoatomic Zintl ions of the group 13 elements are unknown. The inability to produce such complexes has been attributed to the number of electrons, which would be insufficient to stabilize cluster bonding.[1] It might be thought that simple addition of electrons to the clusters could overcome this deficiency; however, this approach runs into electrostatic problems when enough electrons are added to attain a stable bonding situation. Combining group 13 elements with their more electron-rich neighbors to produce heteroatomic Zintl ions, on the other hand, has been successful. Species so-produced include $[TlSn_8]^{4-}$,[2] $[TlSn_9]^{4-}$,[2] and $[Tl_2Te_2]^{2-}$.[3]

It is pertinent to compare these main-group element clusters to some mixed transition-metal/main-group clusters that have been recently characterized. The complex $[SnTe_4]^{4-}$[4] can be compared to $[Bi\{Fe(CO)_4\}_4]^{3-}$,[5] both of which contain a tetrahedrally coordinated central main-group atom and obey the octet rule. More complicated structures represented by $[Bi_4Fe_4(CO)_{13}]^{2-}$[6,7] can be compared to molecules such as $[Bi_4]^{2-}$[8] and $[E_7]^{3-}$ (E = P, As, Sb, and mixed P_4S_3).[9]

In pursuing the ideas that electron-poor main-group elements such as Tl might be incorporated into cluster or cage structures with electron-rich transition-metal fragments, we began exploring the interaction of thallium with iron carbonyls. Some observations in the literature prompted this work. First some poorly defined thallium–iron carbonyls had been reported by Hieber and coworkers in 1959,[10] which suggested such compounds should exist. Thallium–metal carbonyls have been known for some time, but only two structurally characterized examples have been previously reported. $TlCo(CO)_4$[11,12] consists of discrete Tl^+ and $Co(CO)_4^-$ ions. The other compound, $Tl\{CpMo(CO)_3\}_3$,[13] shows a central, essentially planar thallium bonded to three molybdenum atoms in a conventional fashion. Other known but structurally uncharacterized thallium–metal carbonyl compounds are expected to be similar. Further examples include $Tl[Co(CO)_4]_2^-$,[12] $Tl[Co(CO)_4]_3$,[11,14] $[Tl\{Co(CO)_4\}_4]^-$,[15] $Tl[Mn(CO)_5]_3$,[16] and $Tl[(C_5H_4CHPh_2)Cr(CO)_3]$.[17] More recently we have reported the unexpected structure of $[Et_4N]_6[Tl_6Fe_{10}(CO)_{36}]$ obtained from the reaction of $Fe(CO)_5$/KOH/MeOH and $TlCl_3\cdot 4H_2O$.[18] The bonding situation has relationships to both Zintl ion and transition-metal cluster chemistry.

In this paper we present the structural characterization of two related cluster molecules—$[Et_4N]_2[Tl_2Fe_4(CO)_{16}]$ ($[Et_4N]_2[I]$) and $[Et_4N]_4[Tl_4Fe_8(CO)_{30}]$ ($[Et_4N]_4[II]$). These will be compared to the previously reported $[Et_4N]_6[Tl_6Fe_{10}(CO)_{36}]$ ($[Et_4N]_6[III]$).

Experimental Section

The thallium–iron carbonyl complexes described herein are moderately oxygen sensitive, and all manipulations were carried out under an atmosphere of oxygen-free nitrogen by using standard Schlenk and vacuum-line techniques. Organic solvents were distilled before use from standard drying agents, although the complexes are not particularly sensitive to water as evidenced by their isolation from aqueous solution. Infrared spectra were obtained on a PE 1430 spectrophotometer. Analyses were performed by Galbraith Analytical Laboratories (Knoxville, TN). The ^{13}C NMR spectra were measured on a Nicolet 300 spectrophotometer. The reagents $[Et_4N]Br$, $Fe(CO)_5$, Tl_2CO_3, and $TlCl_3\cdot 4H_2O$ were obtained from commercial sources and used without purification.

Synthesis of $[Et_4N]_2[I]$. Pentacarbonyl iron (1.50 g, 7.66 mmol) was added rapidly to a solution of KOH (1.50 g, 26.7 mmol) in MeOH (50 mL) that had been previously prepared and bubbled with N_2. After the mixture was stirred for about 30 min, solid $TlCl_3\cdot 4H_2O$ (1.33 g, 3.47 mmol) was dropped in, at which time the solution color immediately changed from a clear tan to a deep yellow-brown color. Solid Tl_2CO_3

† Rice University.
‡ University of Delaware.
§ Los Alamos National Laboratory.

(1) (a) Corbett, J. D. *Chem. Rev.* **1985**, *85*, 383. (b) Corbett, J. D. *Prog. Inorg. Chem.* **1976**, *21*, 129.
(2) Burns, R. C.; Corbett, J. D. *J. Am. Chem. Soc.* **1982**, *104*, 2804.
(3) Burns, R. C.; Corbett, J. D. *J. Am. Chem. Soc.* **1981**, *103*, 2627.
(4) Huffman, J. C.; Haushalter, J. P.; Umarji, A. M.; Shenoy, G. K.; Haushalter, R. C. *Inorg. Chem.* **1984**, *23*, 2312.
(5) Churchill, M. R.; Fettinger, J. C.; Whitmire, K. H.; Lagrone, C. B. *J. Organomet. Chem.* **1986**, *303*, 99.
(6) Whitmire, K. H.; Churchill, M. R.; Fettinger, J. C. *J. Am. Chem. Soc.* **1985**, *107*, 1056.
(7) Whitmire, K. H.; Albright, T. A.; Kang, S.-K.; Churchill, M. R.; Fettinger, J. C. *Inorg. Chem.* **1986**, *25*, 2799.
(8) Cisar, A.; Corbett, J. D. *Inorg. Chem.* **1977**, *16*, 2482.
(9) (a) Dahlmann, W.; v. Schnering, H. G. *Naturwissenschaften* **1972**, *59*, 420; **1973**, *60*, 429. (b) Schmettow, W.; v. Schnering, H. G. *Angew. Chem., Int. Ed. Engl.* **1977**, *16*, 857. (c) Critchlow, S. C.; Corbett, J. D. *Inorg. Chem.* **1984**, *23*, 770. (d) Adolphson, D. G.; Corbett, J. D.; Merryman, D. J. *J. Am. Chem. Soc.* **1976**, *98*, 7234. (e) Leung, Y. C.; Waser, J.; v. Houten, S.; Vos, A.; Wiegers, G. A.; Wiebenga, E. H. *Acta Crystallogr.* **1957**, *10*, 574.
(10) Hieber, W.; Gruber, J.; Lux, F. *Z. Anorg. Allg. Chem.* **1959**, *300*, 275.
(11) (a) Hieber, W.; Teller, U. *Z. Anorg. Allg. Chem.* **1942**, *249*, 43.
(12) Schussler, D. P.; Robinson, W. R.; Edgell, W. F. *Inorg. Chem.* **1974**, *13*, 153.
(13) Rajaram, J.; Ibers, J. A. *Inorg. Chem.* **1973**, *12*, 1313.
(14) Patmore, D. J.; Graham, W. A. G. *Inorg. Chem.* **1966**, *5*, 1586.
(15) Robinson, W. R.; Schussler, D. P. *J. Organomet. Chem.* **1971**, *30*, C5.
(16) Hsieh, A. T. T.; Mays, M. *J. Organomet. Chem.* **1970**, *22*, 29.
(17) Cooper, R. L.; Fischer, E. O.; Semmlinger, W. *J. Organomet. Chem.* **1967**, *9*, 333.
(18) Whitmire, K. H.; Ryan, R. R.; Wasserman, H. J.; Albright, T. A.; Kang, S.-K. *J. Am. Chem. Soc.* **1986**, *108*, 6831.

0020-1669/88/1327-1347$01.50/0

Table I. Crystallographic Data for $[Et_4N]^+$ Salts of $[I]^{2-}$, $[II]^{4-}$, and $[III]^{6-}$

compd	$[Et_4N]_2[I]$	$[Et_4N]_4[II]$	$[Et_4N]_6[III]$
formula	$C_{32}H_{40}Fe_4N_2O_{16}Tl_2$	$C_{62}H_{80}Fe_8N_4O_{30}Tl_4$	$C_{84}H_{120}Fe_{10}N_6O_{36}Tl_6$
cryst syst	triclinic	monoclinic	monoclinic
space group	$P\bar{1}$	$P2_1/n$	$P2_1/n$
a, Å	11.00 (1)	12.723 (6)	12.266 (5)
b, Å	12.98 (1)	16.077 (6)	20.547 (3)
c, Å	8.77 (1)	21.430 (9)	22.892 (6)
α, deg	105.3 (1)		
β, deg	95.7 (1)	95.97 (4)	93.24 (3)
γ, deg	65.30 (8)		
V, Å^3	1097	4360.2	5759.7
Z	1	2	2
D_{calcd}, g cm^{-3}	2.03	2.00	2.06
μ(Mo Kα), cm^{-1}	87.57	86.4	97.3
temp, K	296	294	298
color	red	black	black
cryst size	0.2 × 0.3 × 0.4	0.2 × 0.3 × 0.3	0.2 × 0.2 × 0.3
diffractometer	Rigaku AFC5S	Nicolet R3m/μ	Enraf-Nonius Cad4
monochromator	graphite	graphite	graphite
radiation	Mo K$\bar{\alpha}$ (λ = 0.709 30 Å)	Mo K$\bar{\alpha}$ (λ = 0.709 30 Å)	Mo K$\bar{\alpha}$ (λ = 0.709 30 Å)
2θ limits, deg	0–55	4–43	0–45
scan type	$\theta/2\theta$	Wyckoff	$\theta/2\theta$
no. of reflcns collcd	5330	5388	7489
no. of indep reflcns	5060	4995	6943
no. of obsd. indep reflcns	3426 ($F_o \geq 6\sigma(F_o)$)	2326 ($F_o \geq 4\sigma(F_o)$)	3079 ($F_o^2 \geq 2\sigma(F_o^2)$)
R(int), %	0.4	4.7	1.4
std reflcns	3 std/147 reflcns (<1% decay)	3 std/97 reflcns (<1% decay)	3 std/1 h (<1% decay)
T_{max}/T_{min}	1.00/0.245	0.027/0.017	1.07/0.82
R,[a] %	5.4	7.8	4.0
R_w,[a] %	8.1	7.8	4.0
$\Delta(\rho)$, e/Å^3	2.7	1.4	1.4

[a] The function minimized during least squares refinement was $\sum w(|F_o| - |F_c|)^2$ where $1/w = \sigma(|F_o|)^2$. R (%) = $100\sum||F_o| - |F_c||/\sum|F_o|$. R_w (%) = $100[\sum w(|F_o| - |F_c|)^2/\sum|F_o|^2]^{1/2}$. The analytical form of the scattering factor for the appropriate neutral atoms was used in calculating F_c values; these were corrected for both the real ($\Delta f'$) and imaginary ($\Delta f''$) components of anomalous dispersion: *International Tables for X-Ray Crystallography*; Kynoch: Birmingham, England, 1974; Vol. 4, pp 99–101, 149–150.

could be used instead of $TlCl_3 \cdot 4H_2O$ except that metallic thallium precipitated over a period of time, indicating that a disproportionation reaction was occurring to give Tl^{3+} as the ion incorporated into the complex in both cases. The $TlCl_3 \cdot 4H_2O$ is, therefore, cleaner and more efficient and is the reagent of choice. The reaction solution was filtered and the product precipitated by addition of $[Et_4N]Br$ (0.729 g, 3.47 mmol) dissolved in H_2O (100 mL). The product was collected by filtration, washed with H_2O, and dried under vacuum. The product is soluble in MeOH, CH_2Cl_2, MeCN, and most polar organic solvents. Yield: 2.19 g, 94.3%. IR (MeOH, cm^{-1}): 1983 m, 1912 s. Anal. Calcd: N, 2.09; Fe, 16.65; Tl, 30.47. Found: N, 1.86; Fe, 15.10; Tl, 30.50. ^{13}C NMR (ppm relative to Me_4Si) 218.0 (carbonyl), 53.3 and 7.6 ($[Et_4N]^+$).

Synthesis of $[Et_4N]_4[II]$. $[Et_4N]_4[II]$ may be prepared by dissolving $[Et_4N]_2[I]$ in MeOH in a quartz tube and irradiating with ultraviolet light overnight. The dark brown product was collected by filtration, washed with CH_2Cl_2, and recrystallized with CH_3CN/MeOH. IR (CH_3CN, cm^{-1}) for $[Et_4N]_4[II]$: 1987 s, 1968 m, sh, 1958 s, 1920 s, sh, 1910 s, 1895 m, sh, 1740 w. Anal. Calcd for $[Et_4N]_4[Tl_4Fe_8(CO)_{30}]$: N, 2.13; Tl, 31.13; Fe, 17.02. Found: N, 1.89; Tl, 30.01; Fe, 17.84.

X-ray Analyses of $[Et_4N]_2[I]$, $[Et_4N]_4[II]$, and $[Et_4N]_6[III]$. For each, the crystals were packed in X-ray quality capillaries and sealed. The crystals were obtained by the following methods: $[Et_4N]_2[I]$ by cooling concentrated CH_2Cl_2 solutions of the complex; $[Et_4N]_4[II]$ by cooling CH_3CN solutions of the complex with MeOH layered on top; $[Et_4N]_6[III]$ from MeOH solution of $[Et_4N]_2[I]$ that was allowed to stand at room temperature for about 1 month. Crystallographic data collection parameters for all three are tabulated in Table I. For $[Et_4N]_2[I]$ the cell parameters and the lack of systematic absences indicated the triclinic space group. The centrosymmetric condition $P\bar{1}$ was chosen and later shown to be correct by successful structure solution. For both $[Et_4N]_4[II]$ and $[Et_4N]_6[III]$ systematic absences uniquely defined the monoclinic space group as $P2_1/n$. All three data sets were corrected for absorption by empirical procedures. The structure for $[Et_4N]_2[I]$ was solved from the Patterson map, that for $[Et_4N]_4[II]$ by direct methods, and that for $[Et_4N]_6[III]$ by heavy-atom techniques. Disordered $[Et_4N]^+$ cations were encountered for both $[Et_4N]_4[II]$ and $[Et_4N]_6[III]$. In $[Et_4N]_4[II]$ it proved impossible to locate reliably any of the cation ethyl group atoms, and their contributions were ignored. The locations of the $[Et_4N]^+$ cations in the lattice are revealed by the found and refined N atom positions. In $[Et_4N]_6[III]$ partial resolution of all cations was possible, and their contributions are included although unrealistic bond

Table II. Atomic Coordinates and Isotropic Thermal Parameters for $[Et_4N]_2[Tl_2Fe_4(CO)_{16}]$

atom	x	y	z	B(eq),[a] Å^2
Tl	−0.03796 (6)	0.10122 (4)	0.19591 (6)	3.30 (3)
Fe(1)	−0.1836 (2)	0.2465 (2)	0.4330 (2)	3.7 (1)
Fe(2)	0.1888 (2)	0.0191 (2)	0.0393 (2)	3.4 (1)
O(1)	−0.403 (1)	0.333 (1)	0.225 (2)	6.2 (8)
O(2)	−0.171 (2)	0.043 (1)	0.526 (2)	10 (1)
O(3)	0.017 (2)	0.343 (2)	0.484 (3)	13 (2)
O(4)	−0.319 (2)	0.413 (1)	0.721 (2)	7.1 (9)
O(5)	0.249 (1)	−0.206 (1)	0.110 (1)	5.5 (8)
O(6)	0.289 (1)	0.142 (1)	0.316 (1)	7 (1)
O(7)	0.043 (1)	0.183 (1)	−0.152 (2)	6 (1)
O(8)	0.430 (1)	−0.077 (1)	−0.154 (2)	8 (1)
N	0.311 (1)	0.351 (1)	0.799 (1)	3.5 (7)
C(1)	−0.315 (1)	0.296 (1)	0.306 (2)	3.8 (7)
C(2)	−0.169 (2)	0.121 (2)	0.491 (2)	7 (1)
C(3)	−0.057 (2)	0.299 (2)	0.458 (3)	8 (1)
C(4)	−0.269 (2)	0.348 (1)	0.605 (2)	5 (1)
C(5)	0.217 (2)	−0.115 (1)	0.079 (2)	4.0 (8)
C(6)	0.246 (2)	0.096 (1)	0.208 (2)	5 (1)
C(7)	0.095 (2)	0.118 (1)	−0.069 (2)	4.3 (9)
C(8)	0.336 (2)	−0.039 (1)	−0.079 (2)	5 (1)
C(11)	0.399 (2)	0.382 (2)	0.715 (3)	6 (1)
C(12)	0.363 (3)	0.385 (2)	0.545 (2)	7 (2)
C(21)	0.311 (2)	0.234 (1)	0.714 (2)	5 (1)
C(22)	0.452 (3)	0.136 (2)	0.686 (3)	8 (2)
C(31)	0.166 (2)	0.440 (2)	0.808 (2)	5 (1)
C(32)	0.141 (2)	0.564 (2)	0.892 (2)	7 (1)
C(41)	0.368 (2)	0.349 (2)	0.965 (2)	5 (1)
C(42)	0.291 (3)	0.321 (2)	1.074 (2)	7 (2)

[a] Equivalent isotropic B defined as one-third of the trace of the orthogonalized $\mathbf{B}_{ij}$ tensor.

metricals and high thermal parameters were encountered. In $[Et_4N]_2[I]$ the cations were ordered and all atoms were refined anisotropically. For $[Et_4N]_4[II]$ and $[Et_4N]_6[III]$ only the thallium and iron positions were refined anisotropically. Programs used for the structure solution of $[Et_4N]_2[I]$ are in the MSC program library, those for $[Et_4N]_4[II]$ are

Table III. Atomic Coordinates ($\times 10^4$) and Isotropic Thermal Parameters ($Å^2 \times 10^3$) for $[Et_4N]_4[Tl_4Fe_8(CO)_{30}]$

atom	x	y	z	U^a
Tl(1)	5185 (1)	5627 (1)	−677 (1)	74 (1)
Tl(2)	6653 (1)	7422 (1)	−1410 (1)	93 (1)
Fe(1)	6158 (4)	5716 (3)	545 (2)	77 (2)
Fe(2)	4659 (5)	6988 (3)	−1395 (3)	87 (3)
Fe(3)	6171 (5)	5857 (3)	−1723 (3)	90 (3)
Fe(4)	8003 (6)	8580 (4)	−1387 (3)	113 (3)
N(1)	616 (62)	7365 (33)	577 (33)	334 (50)
N(2)	5853 (36)	9107 (25)	1754 (21)	199 (24)
O(1)	4240 (20)	6618 (16)	739 (13)	108 (12)
O(2)	7091 (28)	5579 (18)	1863 (13)	166 (17)
O(3)	7340 (23)	7094 (19)	89 (16)	141 (16)
O(4)	7386 (22)	4445 (19)	92 (13)	126 (14)
O(5)	2531 (22)	6441 (20)	−1379 (16)	160 (17)
O(6)	4835 (29)	7984 (16)	−227 (16)	159 (19)
O(7)	4100 (30)	8349 (19)	−2294 (18)	182 (20)
O(8)	4278 (22)	6084 (21)	−2587 (12)	147 (15)
O(9)	8089 (22)	5499 (21)	−956 (15)	145 (17)
O(10)	5546 (31)	4214 (17)	−2053 (14)	155 (19)
O(11)	7213 (26)	6121 (21)	−2827 (13)	143 (17)
O(12)	7301 (34)	9043 (23)	−185 (17)	196 (22)
O(13)	6717 (52)	9279 (31)	−2488 (25)	300 (38)
O(14)	9358 (47)	7313 (33)	−1727 (37)	219 (41)
O(15)	9633 (35)	9885 (23)	−1349 (19)	212 (24)
C(1)	4998 (27)	6225 (19)	620 (16)	71 (14)
C(2)	6728 (30)	5663 (24)	1365 (20)	110 (19)
C(3)	6817 (27)	6472 (25)	271 (16)	90 (18)
C(4)	6877 (31)	4994 (25)	274 (18)	108 (19)
C(5)	3315 (31)	6606 (23)	−1378 (17)	91 (18)
C(6)	4761 (35)	7600 (24)	−660 (23)	125 (22)
C(7)	4411 (42)	7843 (29)	−1979 (26)	120 (26)
C(8)	4815 (33)	6213 (22)	−2132 (16)	98 (18)
C(9)	7314 (27)	5646 (22)	−1247 (19)	92 (17)
C(10)	5745 (34)	4894 (23)	−1913 (18)	109 (19)
C(11)	6794 (26)	6024 (23)	−2415 (16)	81 (16)
C(12)	7638 (35)	8806 (28)	−643 (21)	123 (22)
C(13)	7250 (47)	9008 (41)	−2052 (23)	193 (35)
C(14)	8848 (39)	7755 (26)	−1517 (23)	133 (25)
C(15)	8981 (39)	9404 (28)	−1356 (22)	141 (24)

[a] Equivalent isotropic U defined as one-third of the trace of the orthogonalized U_{ij} tensor.

in the SHELXTL program library, and those for $[Et_4N]_6[III]$ are in the Los Alamos National Laboratory Crystal/Bin program library.

Atomic coordinates for $[Et_4N]_2[I]$, $[Et_4N]_4[II]$, and $[Et_4N]_6[III]$ are given in Tables II–IV, and selected bond distance and angle data are found in Tables V–VIII. Comparative data of related parameters for the anions $[I]^{2-}$, $[II]^{4-}$, and $[III]^{6-}$ are given in Table IX. Additional crystallographic data are available (see supplementary materials paragraph).

Results

When methanolic solutions of $K[HFe(CO)_4]$ generated in situ are treated with thallium salts, the solutions become deep yellow-brown. The same product is obtained with either thallium(III) chloride or with thallium(I) carbonate, but in the case of thallium(I) carbonate a soft, grey precipitate of thallium metal is also obtained. The stoichiometry of that reaction indicates a disproportionation reaction is occurring, so that thallium in the final product is formally Tl(III) starting from either Tl(I) or Tl(III) salts. The complex can be isolated as the tetraethylammonium salt by addition of aqueous $[Et_4N]^+X^-$ (X = Cl, Br). A precipitate is obtained that is soluble in methanol, methylene chloride, and acetonitrile but not in water. Solutions of the compound show a very simple, two-band infrared spectrum in the CO stretching region, and the ^{13}C NMR spectrum has a single peak at room temperature, indicating a very symmetrical compound and/or a fluxional one. Elemental analyses suggested an empirical formula of $[Et_4N][TlFe_2(CO)_8]$ but the compound was later shown by X-ray analysis to be a dimer of that formulation. When allowed to stand for long periods in the solid state or after being placed under vacuum, all of the product would not redissolve in methanol. This can be attributed to the formation of $[Et_4N]_4[II]$ and $[Et_4N]_6[III]$ (see below).

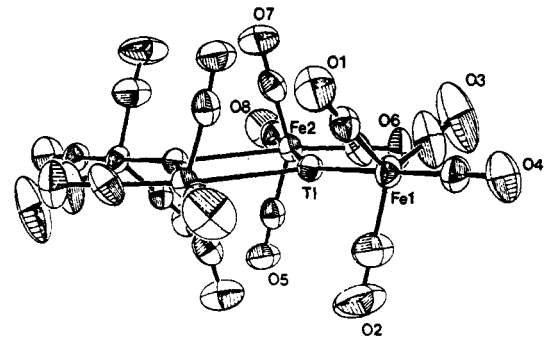

Figure 1. ORTEP diagram and atom-labeling scheme of the anion $[I]^{2-}$, $[Tl_2Fe_4(CO)_{16}]^{2-}$. Carbon atoms are numbered similarly to the oxygens to which they are attached.

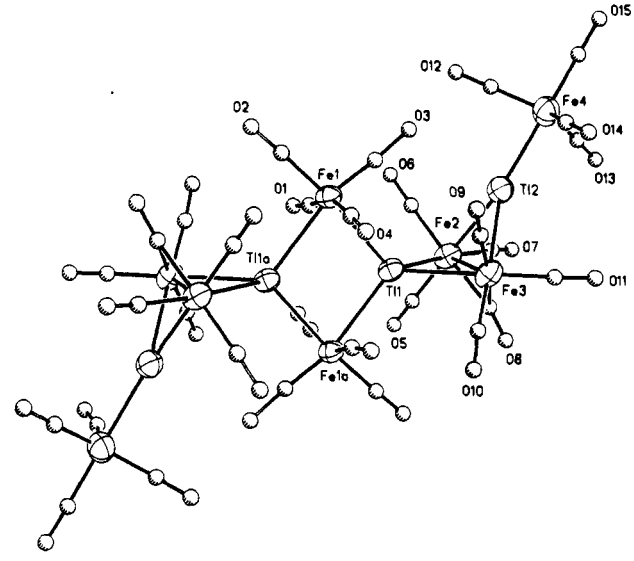

Figure 2. ORTEP diagram and atom-labeling scheme for the anion $[II]^{4-}$, $[Tl_4Fe_8(CO)_{30}]^{4-}$. Carbon atoms are numbered similarly to the oxygens to which they are attached.

Synthesis of $[Et_4N]_4[II]$. When solutions of $[Et_4N]_2[I]$ in methanol are allowed to stand at room temperature for prolonged periods (weeks to months), small black crystals form. X-ray analysis was attempted on a large number of crystals that did not diffract well, but eventually a crystal was found that proved to be $[Et_4N]_6[III]$. Elemental analyses of the bulk material, however, consistently showed a Tl:Fe ratio of 1:2, surprisingly similar to that of $[Et_4N]_2[I]$, which was not expected for $[Et_4N]_6[III]$ (ratio = 3:5). The bulk material was obviously not $[Et_4N]_6[III]$. Closer examination showed that the bulk material was soluble in CH_3CN, and it consistently gave a complex but reproducible infrared spectrum containing a bridging carbonyl band. The color of $[Et_4N]_4[II]$ is not very different from that of $[Et_4N]_2[I]$ in solution. It was then suspected that $[II]^{4-}$ was derived from $[I]^{2-}$ by loss of one CO. Subsequently, it was found that irradiation of solutions of $[Et_4N]_2[I]$ produced $[Et_4N]_4[II]$ much more quickly than simply allowing $[Et_4N]_2[I]$ in methanol to stand at room temperature. The X-ray analysis has shown that $[Et_4N]_4[II]$ has the formation $[Et_4N]_4[Tl_4Fe_8(CO)_{30}]$, which is a dimer of the originally suspected composition. The CO loss is reversible, and in solution, under pressures of CO, $[Et_4N]_4[II]$ is reconverted into $[Et_4N]_2[I]$.

Structures of $[Et_4N]_2[I]$, $[Et_4N]_4[II]$, and $[Et_4N]_6[III]$. All three anions can be viewed as dimers formed around Tl_2Fe_2 parallelograms situated on crystallographic inversion centers (eq 1–3). ORTEP diagrams of the complete anions of $[Et_4N]_2[I]$, $[Et_4N]_4[II]$, and $[Et_4N]_6[III]$ are given in Figures 1–3, respectively, while Figure 4 shows a view of the anions without the carbonyl ligands.

Structural features for all three anions are remarkably similar. Comparative data are found in Table IX. Similarities between

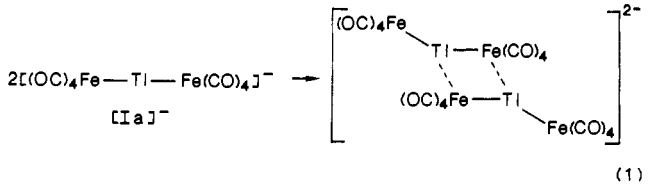

(1)

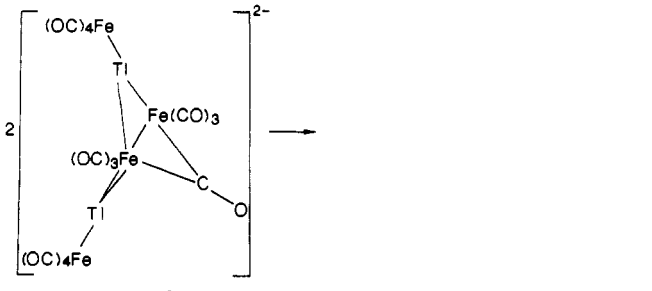

[IIa]$^{2-}$

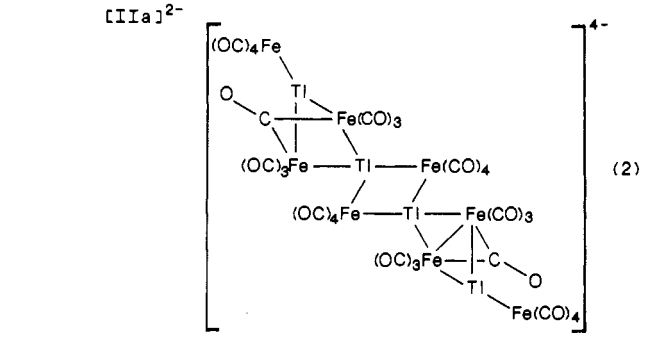

(2)

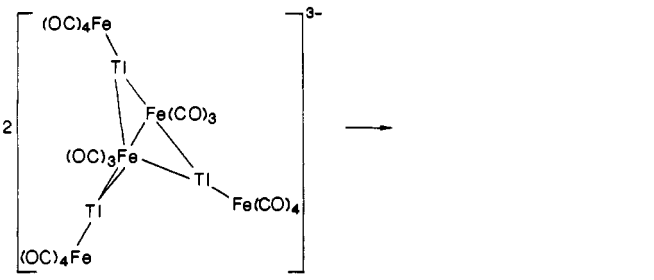

[IIIa]$^{3-}$

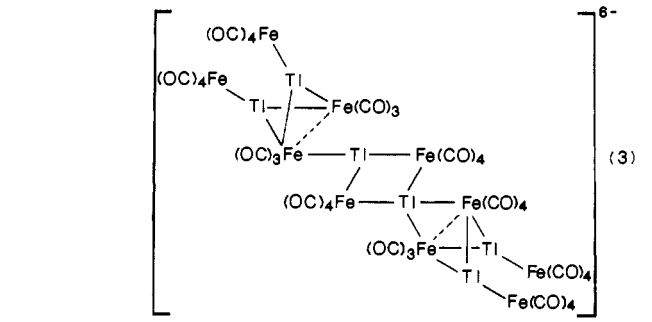

(3)

the structures include the following.

1. The $Fe(CO)_4$ groups in the parallelograms are all distorted cis pseudooctahedra with the CO's, especially the axial ones, tilted toward the Tl_2Fe_2 ring.
2. The terminal $Fe(CO)_4$ groups are trigonal bipyramids with the Tl atoms occupying axial sites. The equatorial CO's of these groups are all tilted slightly toward planar Tl atoms.
3. The Tl–Fe distances become significantly shorter as one moves from the inversion center outwards. The terminal Tl–trigonal-bipyramidal–Fe distances are the shortest Tl–Fe bonds in all three ions: 2.553 (5) Å, $[Et_4N]_2[I]$; 2.530 (7) Å, $[Et_4N]_4[II]$; 2.540 (4)–2.561 (4) Å, $[Et_4N]_6[III]$.
4. No Tl–Tl or Fe–Fe bonds are seen across the Tl_2Fe_2 ring.
5. The nonring Tl–Tl distances in $[II]^{4-}$ and $[III]^{6-}$ are also long (>3.70 Å) and are believed to be nonbonding.
6. All carbonyls except the bridging carbonyl C(8)–O(8) in $[II]^{4-}$ are linear within experimental error.

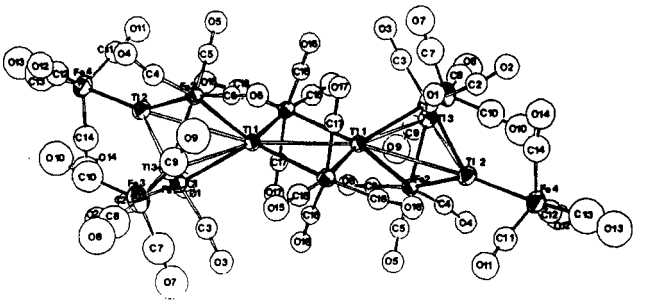

Figure 3. ORTEP diagram and atom-labeling scheme for the anion $[III]^{6-}$, $[Tl_6Fe_{10}(CO)_{36}]^{6-}$. Carbon atoms are numbered similarly to the oxygens to which they are attached.

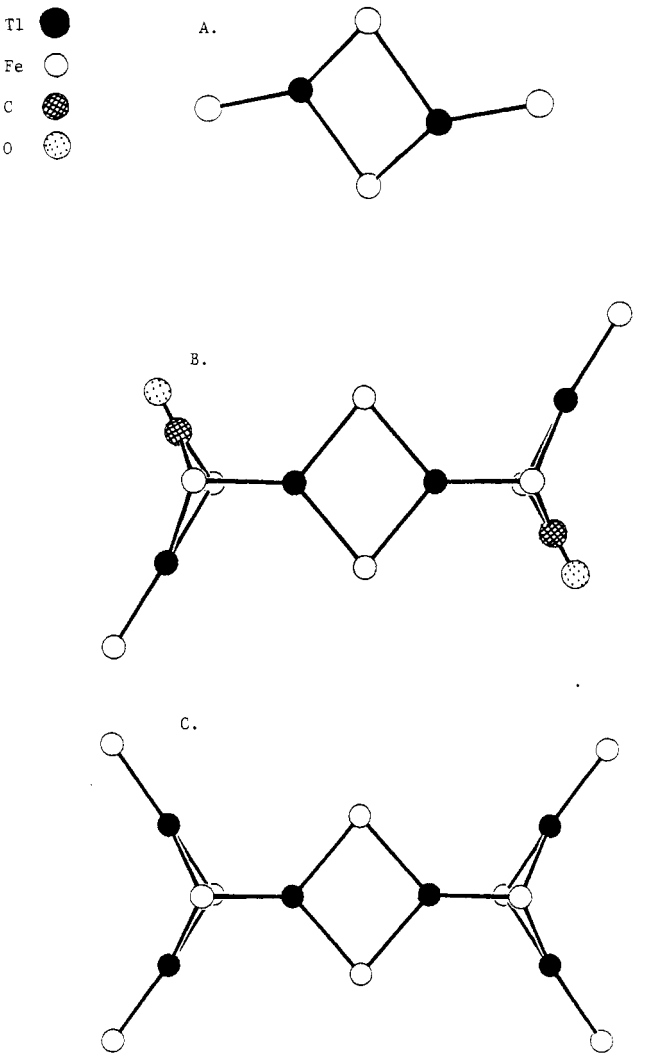

Figure 4. Comparison of the metal frameworks of (a) $[I]^{2-}$, (b) $[II]^{4-}$, and (c) $[III]^{6-}$ viewed perpendicular to the Tl_2Fe_2 parallelograms. Carbonyl ligands have been omitted for clarity.

The Tl's in $[I]^{2-}$ are planar but the angles are severely distorted and asymmetric compared to idealized values. The nonring thallium atoms in $[II]^{4-}$ and $[III]^{6-}$ are also planar, being connected to three Fe's as are the Tl's in $[I]^{2-}$. On the other hand the ring Tl's in $[II]^{4-}$ and $[III]^{6-}$ are four-coordinate severely distorted tetrahedra.

Discussion

The most striking similarity between anions $[I]^{2-}$, $[II]^{4-}$, and $[III]^{6-}$ is that they all contain planar Tl_2Fe_2 parallelograms as the central, structural core of the molecule. In all three cases this central parallelogram can be considered to arise from the dimerization of simpler metal carbonyl fragments as seen in eq 1–3. To arrive at the monomers, the anions are simply cleaved across

Table IV. Atomic Coordinates and Isotropic Thermal Parameters for $[Et_4N]_6[Tl_6Fe_{10}(CO)_{36}]$

atom	*x*	*y*	*z*	*B*, Å^2
Tl(1)	0.01836 (7)	0.94149 (5)	0.93974 (4)	
Tl(2)	0.10596 (8)	0.77553 (5)	0.88968 (4)	
Tl(3)	0.00289 (8)	0.89695 (5)	0.77996 (4)	
Fe(1)	−0.0747 (3)	0.8445 (2)	0.8732 (1)	
Fe(2)	0.1609 (3)	0.8946 (2)	0.8637 (1)	
Fe(3)	−0.0276 (4)	0.9168 (2)	0.6708 (2)	
Fe(4)	0.1566 (3)	0.6555 (2)	0.9045 (2)	
Fe(5)	0.0612 (3)	0.9313 (2)	1.0615 (1)	
C(1)	−0.1015 (19)	0.8093 (10)	0.9380 (10)	5.3 (6)
O(1)	−0.1357 (13)	0.7792 (8)	0.9785 (7)	6.4 (4)
C(2)	−0.1141 (21)	0.7832 (13)	0.8249 (11)	6.6 (7)
O(2)	−0.1544 (15)	0.7434 (9)	0.7947 (8)	8.6 (5)
C(3)	−0.1844 (23)	0.8974 (14)	0.8607 (10)	6.6 (7)
O(3)	−0.2676 (15)	0.9254 (8)	0.8527 (7)	7.6 (5)
C(4)	0.2288 (20)	0.8618 (12)	0.8102 (10)	5.8 (6)
O(4)	0.2919 (14)	0.8415 (8)	0.7749 (7)	7.0 (4)
C(5)	0.2517 (20)	0.8865 (12)	0.9223 (10)	5.6 (6)
O(5)	0.3263 (14)	0.8824 (8)	0.9580 (7)	7.0 (4)
C(6)	0.1741 (17)	0.9749 (12)	0.8445 (9)	4.2 (5)
O(6)	0.1832 (13)	1.0296 (8)	0.8297 (7)	6.5 (4)
C(7)	−0.1547 (36)	0.9343 (19)	0.6849 (15)	12.2 (11)
O(7)	−0.2463 (22)	0.9424 (12)	0.6978 (10)	13.5 (8)
C(8)	−0.0530 (28)	0.9249 (17)	0.5993 (17)	11.8 (11)
O(8)	−0.0636 (21)	0.9347 (13)	0.5474 (12)	14.9 (9)
C(9)	0.0686 (29)	0.9773 (18)	0.6809 (14)	9.7 (10)
O(9)	0.1332 (22)	1.0128 (13)	0.6835 (11)	13.4 (9)
C(10)	0.0238 (30)	0.8381 (20)	0.6635 (15)	11.7 (11)
O(10)	0.0655 (21)	0.7884 (13)	0.6594 (11)	13.9 (9)
C(11)	0.2323 (22)	0.6804 (13)	0.9663 (12)	7.3 (7)
O(11)	0.2848 (16)	0.6940 (9)	1.0108 (8)	9.7 (6)
C(12)	0.2115 (23)	0.6635 (14)	0.8362 (13)	7.8 (8)
O(12)	0.2471 (16)	0.6710 (10)	0.7901 (8)	9.2 (6)
C(13)	0.1806 (41)	0.5698 (26)	0.9133 (21)	16.9 (18)
O(13)	0.2063 (25)	0.5231 (16)	0.9189 (13)	16.5 (11)
C(14)	0.0118 (28)	0.6447 (15)	0.9139 (12)	8.9 (9)
O(14)	−0.0778 (19)	0.6339 (10)	0.9190 (9)	10.7 (7)
C(15)	0.0780 (20)	0.9362 (13)	1.1343 (11)	6.4 (6)
O(15)	0.0917 (14)	0.9438 (9)	1.1863 (8)	8.3 (5)
C(16)	0.1750 (19)	0.9759 (11)	1.0417 (9)	4.5 (6)
O(16)	0.2567 (13)	1.0028 (7)	1.0311 (6)	5.7 (4)
C(17)	−0.0792 (20)	0.9140 (11)	1.0550 (9)	4.7 (6)
O(17)	−0.1709 (13)	0.9003 (8)	1.0547 (6)	6.0 (4)
C(18)	0.1149 (20)	0.8525 (13)	1.0459 (10)	5.9 (6)
O(18)	0.1363 (14)	0.8009 (9)	1.0333 (7)	7.0 (5)
N(1)	0.9624 (21)	0.6744 (13)	0.1270 (11)	9.2 (7)
C(19)	1.0287 (26)	0.6641 (15)	0.1832 (13)	9.5 (9)
C(20)	1.1338 (32)	0.7045 (18)	0.1847 (15)	13.7 (12)
C(21)	0.9193 (25)	0.7462 (16)	0.1192 (13)	9.9 (9)
C(22)	0.8616 (25)	0.7748 (15)	0.1710 (13)	9.9 (9)
C(23)	0.8567 (24)	0.6316 (13)	0.1316 (12)	8.3 (8)
C(24)	0.7731 (26)	0.6377 (15)	0.0803 (13)	10.1 (9)
C(25)	1.0172 (22)	0.6570 (14)	0.0680 (12)	7.7 (8)
C(26)	1.0545 (22)	0.5872 (14)	0.0733 (11)	8.2 (8)
N(2)	0.5297 (23)	0.0805 (14)	0.8269 (12)	10.6 (8)
C(27)	0.5332 (35)	0.1506 (21)	0.8289 (17)	14.9 (14)
C(28)	0.6415 (30)	0.1704 (18)	0.8687 (15)	13.4 (12)
C(29)	0.5225 (34)	0.0352 (21)	0.8763 (19)	14.8 (13)
C(30)	0.4438 (32)	0.0652 (19)	0.9182 (17)	14.7 (13)
C(31)	0.4313 (28)	0.0756 (17)	0.7798 (14)	11.4 (10)
C(32)	0.4228 (33)	−0.0045 (20)	0.7611 (16)	15.0 (13)
C(33)	0.6298 (36)	0.0568 (21)	0.7914 (20)	16.3 (14)
C(34)	0.6432 (32)	0.0824 (20)	0.7299 (18)	15.7 (14)
N(3)	0.9337 (29)	0.1979 (17)	0.5986 (14)	12.8 (10)
C(35)	0.9950 (45)	0.2021 (28)	0.5477 (24)	21.8 (21)
C(36)	0.9338 (31)	0.2531 (18)	0.5012 (16)	14.1 (13)
C(37)	0.8974 (38)	0.2570 (26)	0.6260 (19)	17.7 (17)
C(38)	0.9874 (30)	0.3106 (19)	0.6385 (15)	12.9 (12)
C(39)	1.0104 (40)	0.1649 (23)	0.6457 (22)	18.5 (17)
C(40)	0.9396 (33)	0.1468 (18)	0.6991 (17)	14.3 (13)
C(41)	0.8250 (32)	0.1592 (20)	0.5840 (16)	13.0 (12)
C(42)	0.8666 (34)	0.0948 (22)	0.5662 (17)	16.0 (14)

the Tl_2Fe_2 parallelograms. These hypothetical monomers are shown as $[Ia]^-$, $[IIa]^{2-}$, and $[IIIa]^{3-}$, respectively.

These monomers may have more than a theoretical existence. This is illustrated for $[Et_4N]_2[I]$, which shows only a single ^{13}C NMR signal at room temperature in CD_2Cl_2 solution. The dimeric form $[I]^{2-}$ should possess at least two carbonyl ^{13}C NMR signals—one for carbonyls on the bridging, pseudooctahedral irons and one for carbonyls on the terminal, trigonal-bipyramidal irons.

Table V. Selected Bond Distances and Angles for $[Et_4N]_2[Tl_2Fe_4(CO)_{16}]$

(a) Bond Distances (Å)			
Tl–Fe(1)	2.553 (5)	Tl–Fe(2)	2.632 (5)
Tl–Fe(2a)	3.038 (4)	Tl···Tl(a)	3.658 (5)
Fe···Fe(2a)	4.352 (5)		
(b) Bond Angles (deg)			
Fe(1)–Tl–Fe(2)	147.2 (1)	Fe(2)–Tl–Fe(2a)	100.0 (1)
Fe(1)–Tl–Fe(2a)	112.3 (1)	Tl–Fe(2)–Tl(a)	80.0 (1)

Table VI. Selected Bond Distances and Angles for $[Et_4N]_4[Tl_4Fe_8(CO)_{30}]$

(a) Bond Distances (Å)			
Tl(1)···Tl(2)	3.859 (2)	Tl(2)–Fe(2)	2.635 (6)
Tl(1)···Tl(1a)	3.604 (3)	Tl(2)–Fe(3)	2.658 (6)
Tl(1)–Fe(1)	2.781 (5)	Tl(2)–Fe(4)	2.530 (7)
Tl(1)–Fe(1a)	2.786 (6)	Fe(2)–Fe(3)	2.788 (8)
Tl(1)–Fe(2)	2.718 (6)	Fe(2)–C(8)	2.04 (4)
Tl(1)–Fe(3)	2.706 (6)	Fe(3)–C(8)	1.94 (4)
(b) Bond Angles (deg)			
Fe(1)–Tl(1)–Fe(1a)	99.3 (1)	Tl(1)–Fe(1)–Tl(1a)	80.7 (1)
Fe(1)–Tl(1)–Fe(2)	123.4 (2)	Tl(1)–Fe(2)–Tl(2)	92.3 (2)
Fe(1)–Tl(1)–Fe(3)	125.0 (2)	Tl(1)–Fe(3)–Tl(2)	92.0 (2)
Fe(1a)–Tl(1)–Fe(2)	124.3 (2)	Tl(2)–Fe(2)–Fe(3)	58.9 (2)
Fe(1a)–Tl(1)–Fe(3)	122.2 (2)	Tl(1)–Fe(3)–Fe(2)	59.3 (2)
Fe(2)–Tl(2)–Fe(4)	147.9 (2)	Tl(2)–Fe(2)–Fe(3)	58.6 (2)
Fe(3)–Tl(2)–Fe(4)	147.1 (2)	Tl(2)–Fe(3)–Fe(2)	57.8 (2)

Table VII. Selected Bond Distances and Angles for $[Et_4N]_6[Tl_6Fe_{10}(CO)_{36}]$

(a) Bond Distances (Å)			
Tl(1)···Tl(1′)	3.706 (1)	Tl(2)–Fe(1)	2.639 (3)
Tl(1)···Tl(2)	3.773 (1)	Tl(2)–Fe(2)	2.615 (4)
Tl(1)···Tl(3)	3.765 (1)	Tl(2)–Fe(4)	2.561 (4)
Tl(2)···Tl(3)	3.711 (1)	Tl(3)–Fe(1)	2.617 (3)
Tl(1)–Fe(1)	2.721 (3)	Tl(3)–Fe(2)	2.648 (3)
Tl(1)–Fe(2)	2.713 (3)	Tl(3)–Fe(3)	2.540 (4)
Tl(1)–Fe(5)	2.790 (4)	Fe(1)···Fe(2)	3.087 (5)
Tl(1)–Fe(5′)	2.815 (3)		
(b) Bond Angles (deg)			
Fe(1)–Tl(1)–Fe(2)	69.2 (1)	Fe(1)–Tl(3)–Fe(3)	146.0 (1)
Fe(1)–Tl(1)–Fe(5)	123.0 (1)	Fe(2)–Tl(3)–Fe(3)	140.9 (1)
Fe(1)–Tl(1)–Fe(5′)	123.3 (1)	Tl(1)–Fe(1)–Tl(2)	89.5 (1)
Fe(2)–Tl(1)–Fe(5)	124.4 (1)	Tl(1)–Fe(1)–Tl(3)	89.7 (1)
Fe(2)–Tl(1)–Fe(5′)	122.1 (2)	Tl(2)–Fe(1)–Tl(3)	89.8 (1)
Fe(5)–Tl(1)–Fe(5′)	97.2 (1)	Tl(1)–Fe(2)–Tl(2)	90.2 (1)
Fe(1)–Tl(2)–Fe(2)	72.0 (1)	Tl(1)–Fe(2)–Tl(3)	89.2 (1)
Fe(1)–Tl(2)–Fe(4)	137.0 (1)	Tl(2)–Fe(2)–Tl(3)	89.7 (1)
Fe(2)–Tl(2)–Fe(4)	150.1 (1)	Tl(1)–Fe(5)–Tl(1′)	82.8 (1)
Fe(1)–Tl(3)–Fe(2)	71.8 (1)		

Table VIII. Dihedral Angles (deg) for $[Et_4N]_4[Tl_4Fe_8(CO)_{30}]$ and $[Et_4N]_6[Tl_6Fe_{10}(CO)_{36}]$

(a) $[Tl_4Fe_8(CO)_{30}]^{4-}$			
plane A	Tl(1), Fe(1), Tl(1a), Fe(1a)		
plane B	Tl(1), Fe(2), Fe(3)		
plane C	Fe(2), Fe(3), Tl(2)		
A–B	88.0 (1)	B–C	115.0 (1)
A–C	89.7 (1)		
(b) $[Tl_6Fe_{10}(CO)_{36}]^{6-}$			
plane A	Tl(1), Fe(5), Tl(1′), Fe(5′)		
plane B	Fe(1), Fe(2), Tl(1)		
plane C	Fe(1), Tl(2), Fe(2)		
plane D	Fe(1), Fe(2), Tl(3)		
plane E	Tl(1), Tl(2), Tl(3)		
A–B	91.7 (1)	B–E	90.7 (1)
A–E	1.0 (1)	C–D	58.8 (1)
B–C	60.2 (1)	C–E	90.5 (1)
B–D	119.0 (1)	D–E	89.8 (1)

Table IX. Comparison of Structural Parameters of the Tl_2Fe_2 Parallelograms of $[Et_4N]_2[I]$, $[Et_4N]_4[II]$, and $[Et_4N]_6[III]$[a]

compd	α, deg	β, deg	γ, deg	δ, deg	a, Å	b, Å	c, Å	d, Å
$[Et_4N]_2[I]$	97.1 (8)	144.4 (7)	80.0 (1)	100.0 (1)	2.632 (5)	3.038 (4)	3.658 (5)	4.352 (5)
$[Et_4N]_4[II]$	102.3 (17)	154.2 (18)	80.7 (1)	99.3 (1)	2.781 (5)	2.786 (6)	3.604 (3)	4.243 (8)
$[Et_4N]_6[III]$	103 (1)	151 (1)	82.8 (1)	97.2 (1)	2.790 (4)	2.815 (3)	3.706 (1)	4.205 (5)

[a] Parameters are defined by

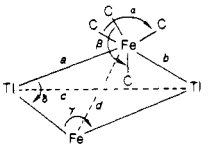

More signals might be anticipated if the fluxionality of the carbonyls is low. The important point is that dimer $[I]^{2-}$ should have at least two ^{13}C NMR signals for the carbonyls and only one is observed. In contrast, the monomer $[Ia]^-$ would be expected to show one ^{13}C signal. It is, therefore, believed that $[I]^{2-}$ exists as a monomer in solution. The structural parameters for $[I]^{2-}$ support this hypothesis. Two of the Tl–Fe distances (crystallographically equivalent) are very long—3.038 (4) Å compared to the other unique Tl–Fe distance in the parallelogram of 2.632 (5) Å. Additionally, the angles about thallium are not symmetrical. Since the Fe(2)–Tl–Fe(2a) angle is 100.0 (1)°, symmetrical displacement of the external $Fe(CO)_4$ group would require ∠Fe(1)–Tl–Fe(2) and ∠Fe(1)–Tl–Fe(2a) to be equal and to be 130°. The angles in question are 147.2 (1)° and 112.3 (1)°. The structural parameters strongly suggest that $[I]^{2-}$ is a weakly dimerized form of $[Ia]^-$.

The solution infrared spectrum of $[Et_4N]_2[I]$ is quite simple and similar to spectra we have encountered for other $Fe(CO)_4L$-type complexes, again an indication that the monomer exists in solution. The dimer would require more bands due to the lower symmetry added by the presence of both octahedral and trigonal-bipyramidal $Fe(CO)_4$ groups.

Structurally characterized literature precedents exist for $[Ia]^-$. These molecules are the isoelectronic $[Na(THF)_2]_2[M\{Fe(CO)_4\}_2]$ (THF = tetrahydrofuran; M = Zn, Cd, Hg).[19] A structural feature of these molecules that persists in the thallium–iron clusters $[I]^{2-}$, $[II]^{4-}$, and $[III]^{6-}$ is a noticeable tilting of the equatorial carbonyls on trigonal-bipyramidal metals toward the post-transition-metal/main-group atom.

The dimeric form $[I]^{2-}$ has a literature precedent in $Fe_2(CO)_8[\mu\text{-}InMn(CO)_5]_2$.[20] This neutral molecule can be derived by replacing the $\{\mu\text{-}TlFe(CO)_4\}^-$ fragments of $[I]^{2-}$ with isoelectronic $\{\mu\text{-}InMn(CO)_5\}$ groups. In that molecule the Fe_2In_2 parallelogram is much more symmetric with the unique Fe–In distances being 2.662 (1) Å and 2.663 (1) Å. The In–In distance (3.250 (1) Å) and Fe–Fe distance (4.218 (1) Å) are nonbonding as expected. Other structurally related molecules that possess two fewer electrons but have a metal–metal bond across an M_2E_2 parallelogram include $M_2(CO)_8\{\mu\text{-}EM(CO)_5\}_2$ {M = Mn or Re; E = Ga or In}.[21] Larger ring systems are observed for $[Fe(CO)_4Cd]_4$[22] and $[Fe(CO)_4Cd(bpy)]_3$.[23] Just as the trigonal-bipyramidal equatorial carbonyls are tilted toward the main-group atoms in these molecules, so the CO ligands on the octahedral iron atoms are very strongly tilted toward the center of the ring system for $[I]^{2-}$, $[II]^{4-}$, and $[III]^{6-}$.

In drawing simple electron dot diagrams of these molecules, one immediately predicts thallium to be electron deficient. Normally, a main-group element would be most happy with a filled octet of electrons, or six electrons for group 13 elements, but $[Ia]^-$ obviously has only four electrons about thallium. This electron deficiency can be relieved in part by dimerization. If the bridging $Fe(CO)_4$ groups share electrons rather than act as simple electron pair acceptors, the thallium can obtain a six-electron configuration. Clearly for $[Et_4N]_2[I]$ the sharing of electrons is not complete as indicated by the crystal structure bond parameters, but we believe this process to be important in building up these oligomeric structures. The dimerization for $[Et_4N]_4[II]$ and $[Et_4N]_6[III]$ appears somewhat stronger from their bond parameters. The electron deficiency can also be alleviated by interaction of the electropositive Tl atoms and the π clouds of the CO ligands, which is consistent with the experimentally observed tilting of these ligands discussed in the preceding paragraph.

Table X. Comparison of Selected Fe–Fe Distances in Molecules Related to $[Et_4N]_4[II]$ and $[Et_4N]_6[III]$

compd	d_{Fe-Fe}, Å	ref
$Fe_2(CO)_9$	2.523 (1)	31
$[PPN]_2[Fe_2(CO)_8]\cdot 2CH_3CN$	2.787 (2)	32
$[Et_4N]_2[Pb\{Fe_2(CO)_8\}\{Fe(CO)_4\}_2]$	2.617 (5)	33
$Pb[Fe_2(CO)_8]_2$	2.900 (av)	26
$Sn[Fe_2(CO)_8]_2$	2.87	26
$Ge[Fe_2(CO)_8]_2$	2.823 (av)	26
$Fe_2(CO)_6[\mu\text{-}GeMe_2]_3$	2.750 (11)	27

Loss of CO from $[I]^{2-}$ can easily be envisioned as leading to $[IIa]^{2-}$, which can then dimerize giving $[II]^{4-}$ (eq 2). The monomer $[IIa]^{2-}$ is isoelectronic with $Fe_2(CO)_9$ and can be derived from that molecule by replacing two bridging carbonyls with $[\mu\text{-}TlFe(CO)_4]^-$ groups. Perhaps a better comparison could be made to isoelectronic $Co_2(CO)_6(\mu\text{-}CO)[\mu\text{-}ZnCo(CO)_4]_2$, which has been prepared by Burlitch and co-workers.[24] The bridging CO of $[IIa]^{2-}$ persists in CH_3CN solution as evidenced by an infrared band at 1740 cm^{-1}. In fact, the infrared spectrum of $[Et_4N]_4[II]$ dissolved in CH_3CN is remarkably similar to that of $Co_2(CO)_6(\mu\text{-}CO)[\mu\text{-}ZnCo(CO)_4]_2$. We expect $[II]^{4-}$ to dissociate to monomer $[IIa]^{2-}$ in solution. The symmetry of the dimer would be lower than that for $[IIa]^{2-}$ and more bands would be expected. The solid-state infrared spectrum in contrast is much more complicated and appears almost as a continuum from 2000 to about 1850 cm^{-1}.

The dimerization of $[IIa]^{2-}$ to give $[II]^{4-}$ is similar in nature to that observed for $[Ia]^-$ to $[I]^{2-}$. The coupling of the molecules occurs via side on interaction of two $Tl\text{–}Fe(CO)_4$ groups in adjacent molecules. The result is a similar Tl_2Fe_2 parallelogram showing the same distortion of the octahedral environment about iron as in $[Et_4N]_2[I]$ (Table IX). The tetrahedrally coordinated thalliums in $[Et_4N]_4[II]$, however, would more closely attain an octet of electrons.

The Fe–Fe distance of 2.788 (8) Å in $[II]^{4-}$ is long but does fall within the range of Fe–Fe distances observed in other related clusters. Table X contains a listing of Fe–Fe distances for comparison. It should be remembered that the bridging group has an effect on the metal–metal bond length. Bridging carbonyl ligands are associated with a shortening of metal–metal bond distance, while large main-group atoms would be expected to cause a lengthening of the bond.[25] This is clearly seen for the iso-

(19) Sosinsky, B. A.; Shong, R. G.; Fitzgerald, B. J.; Norem, N.; O'Rourke, C. *Inorg. Chem.* **1983**, *22*, 3124.
(20) Preut, H.; Haupt, H.-J. *Acta Crystallogr., Sect. B: Struct. Crystallogr. Cryst. Chem.* **1979**, *35*, 2191.
(21) (a) Preut, H.; Haupt, H.-J. *Chem. Ber.* **1974**, *107*, 2860; **1975**, *108*, 1447. (b) Haupt, H.-J.; Neumann, F. *J. Organomet. Chem.* **1974**, *74*, 185.
(22) Ernst, R. D.; Marks, T. J.; Ibers, J. A. *J. Am. Chem. Soc.* **1977**, *99*, 2090.
(23) Ernst, R. D.; Marks, T. J.; Ibers, J. A. *J. Am. Chem. Soc.* **1977**, *99*, 2098.
(24) Burlitch, J. M.; Hayes, S. E.; Lemley, J. T. *Organometallics* **1985**, *4*, 167.
(25) Whitmire, K. H.; Lagrone, C. B.; Churchill, M. R.; Fettinger, J. C.; Biondi, L. V. *Inorg. Chem.* **1984**, *23*, 4227.

electronic, isostructural series $E\{Fe_2(CO)_8\}_2$, where E = Ge, Sn, and Pb, respectively.[26] Thus the bond distance in $[II]^{4-}$ represents a value that results from opposing forces: the two bridging thallium atoms would tend to lengthen the Fe–Fe distance while the μ-CO would tend to contract that bond. With both types of interaction present in $[II]^{4-}$ it is impossible to separate the effects. This issue is also important for $[Et_4N]_6[III]$.

Anion $[III]^{6-}$ can most conveniently be considered to be a dimer of $[Fe_2(CO)_6\{\mu\text{-}TlFe(CO)_4\}_3]^{3-}$, $[IIIa]^{3-}$, which is isoelectronic with $Fe_2(CO)_9$ It is formally derived from $Fe_2(CO)_9$ by replacement of all three bridging CO's with $\{TlFe(CO)_4\}^-$ fragments. A structural characterization of a related molecule, $Fe_2(CO)_6(\mu\text{-}GeMe_2)_3$,[27] has been previously reported. An important feature of this molecule, as evidenced by the structure of $[III]^{6-}$, is the long Fe–Fe distance, 3.087 (5) Å, which is ca. 0.19 Å longer than the longest previously known Fe–Fe bonding distance. This value indicates a lack of direct metal–metal interaction, but that is not necessarily problematic in light of molecular orbital calculations.[18] Previous studies on simpler bridged systems indicated that the bonding in this class of molecule primarily occurs through the bridge interactions.[28] Molecular orbital calculations on $[IIIa]^{3-}$ confirmed this, supporting a diamagnetic configuration that showed a very low Fe–Fe overlap population. Thus the characterization of stable $[Et_4N]_6[III]$ with a clearly nonbonding Fe–Fe distance stands as experimental confirmation of the theoretical postulate that the bonding in these molecules occurs primarily through the bridge interactions.

Dimerization of $[IIIa]^{3-}$ to give $[III]^{6-}$ is qualitatively the same as for $[Ia]^-$ and $[IIa]^{2-}$ (see Table IX) with like distortion of the consequently formed pseudooctahedral $Fe(CO)_4$ groups.

One feature that should be noted for all anions $[I]^{2-}$, $[II]^{4-}$, and $[III]^{6-}$ is that the Tl···Tl distances across the parallelograms are long (3.604 (3)–3.706 (1) Å) and probably do not represent bonding interactions in the conventional sense. It is interesting to note, however, that these distances are only a few tenths of an ångstrom longer than the Tl–Tl distances in the α form (room temperature) of elemental thallium: 3.4076 and 3.4566 Å. Other Tl···Tl distances in $[II]^{4-}$ and $[III]^{6-}$ are longer than the values between thalliums within the parallelograms. In $[II]^{4-}$, Tl(1)···Tl(2) is 3.859 (2) Å, while in $[III]^{6-}$ three other long Tl···Tl distances are present: Tl(1)···Tl(2), 3.773 (1) Å; Tl(1)···Tl(3), 3.765 (1) Å, and Tl(2)···Tl(3), 3.711 (1) Å. It is of interest to compare these distances to those observed between main-group atoms in the organic conducting materials $(TMTSF)_2X$ (TMTSF = tetramethyltetraselenafulvalene; X = $[PF_6]^-$, $[ClO_4]^-$, $[ReO_4]^-$).[29] For those complexes Se–Se distances along the stacks of TMTSF groups range between 3.874 and 4.138 Å.

The Tl–Fe distances show some consistent features for all three anions. The shortest Tl–Fe contacts are those between thallium atoms and "terminal", trigonal-bipyramidal irons. These distances are all under 2.57 Å: $[Et_4N]_2[I]$, Tl(1)–Fe(1) = 2.553 (5) Å; $[Et_4N]_4[II]$, Tl(2)–Fe(4) = 2.530 (7) Å; $[Et_4N]_6[III]$, Tl(2)–Fe(4) = 2.561 (4) Å and Tl(3)–Fe(3) = 2.540 (4) Å. These bonds are best described as two-electron-donor bonds from Tl–Fe. In light of recent work by Herrmann and co-workers, which has indicated multiple bonding between main-group atoms and transition metals,[30] multiple bonding may be present in these Tl–terminal $Fe(CO)_4$ bonds. That would further alleviate the electron deficiency at the thallium center. In considering the possibility of multiple bonding, an obvious connection to the isolobal analogy can be made. As a reviewer has pointed out, C_{2v} $Fe(CO)_4$ is isolobal with CH_2 and Tl^- with C. Thus the simplest case, $[(OC)_4Fe\text{–}Tl\text{–}Fe(CO)_4]^-$, can be viewed as an analogue to allene, $H_2C{=}C{=}CH_2$. A problem with this view is that the symmetry around the $Fe(CO)_4$ is expected to be C_{3v} (trigonal bipyramidal, Tl axial) and not C_{2v} (trigonal bipyramidal, Tl equatorial) (cf. $[E\{Fe(CO)_4\}_2]^{2-}$ (E = Cd, Zn, Hg)).[19] The π bonding between the metal and the thallium would be at a minimum for the C_{3v} configuration since the π back-bonding is maximal for the equatorial site. This is seen in the preference for ligands with strong π-accepting capabilities such as ethylene fitting in equatorial sites in $Fe(CO)_4$ complexes, while weaker π acceptors such as phosphines prefer the axial sites.

The next longest Tl–Fe distances are those bonds best described as "covalent" bonds to three-coordinate thallium. In $[Et_4N]_4[II]$ these values range from 2.635 (6) to 2.658 (6) Å, while in $[Et_4N]_6[III]$ they range from 2.615 (4) to 2.648 (3) Å. The longest Tl–Fe bonds for both $[Et_4N]_4[II]$ and $[Et_4N]_6[III]$ are those "covalent" bonds to four-coordinate thallium. These distances range from 2.706 (6) to 2.786 (6) Å in $[Et_4N]_4[II]$ and from 2.713 (3) to 2.815 (3) Å in $[Et_4N]_6[III]$. These trends in bond length follow very nicely the expected areas of electron deficiency in the cluster molecules.

Acknowledgment. The National Science Foundation (Grant CHE 8421217), the donors of Petroleum Research Fund, administered by the American Chemical Society, and the Robert A. Welch Foundation are gratefully acknowledged for the support of this work. Associated Western Universities is also thanked for support that allowed the crystallographic study on $[Et_4N]_6[Tl_6Fe_{10}(CO)_{36}]$ to be carried out at Los Alamos National Laboratory.

Registry No. $[Et_4N]_2[I]$, 113218-98-7; $[Et_4N]_4[II]$, 113218-96-5; $[Et_4N]_6[III]$, 104337-76-0; $Fe(CO)_5$, 13463-40-6; Fe, 7439-89-6; Tl, 7440-28-0.

Supplementary Material Available: For $[Et_4N]_2[Tl_2Fe_4(CO)_{16}]$, $[Et_4N]_4[Tl_4Fe_8(CO)_{30}]$, and $[Et_4N]_6[Tl_6Fe_{10}(CO)_{36}]$, listings of anisotropic thermal parameters and complete bond distances and angles (11 pages); tables of calculated and observed structure factors for all three complexes (63 pages). Ordering information is given on any current masthead page.

(26) (a) Melzer, D.; Weiss, E. *J. Organomet. Chem.* **1983**, *255*, 335. (b) Lindley, P. F.; Woodward, P. *J. Chem. Soc. A* **1967**, 382. (c) Whitmire, K. H.; Lagrone, C. B.; Churchill, M. R.; Fettinger, J. C.; Robinson, B. H. *Inorg. Chem.* **1987**, *26*, 3491.
(27) Elder, M.; Hall, D. *Inorg. Chem.* **1969**, *8*, 1424.
(28) (a) Summerville, R. H.; Hoffmann, R. *J. Am. Chem. Soc.* **1979**, *101*, 3821. (b) Bauschlicher, C. W., Jr. *J. Chem. Phys.* **1986**, *84*, 872.
(29) Thorup, N.; Rindorf, G.; Soling, H. *Phys. Scr.* **1982**, *25*, 868.
(30) Herrmann, W. A. *Angew. Chem.* **1986**, *98*, 57.
(31) Cotton, F. A.; Troup, J. M. *J. Chem. Soc., Dalton Trans.* **1974**, 800.
(32) Chin, H. B.; Smith, M. B.; Wilson, R. D.; Bau, R. *J. Am. Chem. Soc.* **1974**, *96*, 5285.
(33) Lagrone, C. B.; Whitmire, K. H.; Churchill, M. R.; Fettinger, J. C. *Inorg. Chem.* **1986**, *25*, 2080.